

# Performance and Numerical Analysis of Single Basin Solar Still Integrated with and without Salt Gradient Solar Pond

Ni Ni Aung <sup>a</sup>, Myat Myat Soe <sup>b</sup>

<sup>a</sup>Department of Mechanical Engineering, Mandalay Technological University, The Republic of the Union of Myanmar

<sup>b</sup>Department of Mechanical Engineering, Mandalay Technological University, The Republic of the Union of Myanmar

<sup>a</sup>Email: [angelkalay123@gmail.com](mailto:angelkalay123@gmail.com)

<sup>b</sup>Email: [myatmyatsoe.mtu@gmail.com](mailto:myatmyatsoe.mtu@gmail.com)

**Abstract-** The productivity of distilled water is directly proportional to water temperature in solar still. In this work, a single basin single slope solar still is integrated with a salt gradient solar pond (SGSP) to increase the productivity of solar still. The performance of the single basin single slope solar still integrated with and without salt gradient solar pond has been analyzed theoretically, numerically and experimentally. The energy balance equations have been written for different temperature elements of the solar still and solar pond. Here, a two-phase three-dimensional model was made for evaporation as well as condensation process in solar still by using ANSYS CFX method to simulate the present model. The experiments with single basin solar still have been carried out from June to October 2017. The highest temperature of thermal storage zone reached 312 K. On September 21<sup>st</sup> 2017, the storage zone temperature is occurred 310.3 K, 310.16 K and 309.5 K according to the numerical simulation, theory calculation and experimental measurements of SGSP. The water temperature in single basin solar still integrated with salt gradient solar pond is 343.4 K, 343.3 K, 343 K and without solar pond is 312 K, 312 K, 311.9 K according to the simulation, theory, and experiment at 12 pm of September 21<sup>st</sup> 2017. Distilled water productivity of solar still integrated with SGSP is 0.000050 kg/s, 0.000049 kg/s, 0.0000487 kg/s and without solar pond is 0.000042 kg/s, 0.000041 kg/s, 0.00004 kg/s. The average productivity of single basin solar still with salt gradient solar pond is 40.78 % higher than solar still without solar pond. The maximum daily efficiency of the solar still coupled with and without solar pond was found to be 8.00 % and 5.04 %. Simulation and theoretical results of single basin solar still also show a good agreement with experimental results.

*Index Terms-* desalination, distilled water productivity, salt gradient solar pond, single basin solar still, solar energy

## I. INTRODUCTION

Water is one of the most abundant resources on earth, covering three-fourths of the planet's surface. About 97% of the earth's water is salt water in the oceans; 3% of all fresh water is in ground water, lakes and rivers, which supply most of human and animal needs. Most water resources contain salt, bacteria and pollutants. Apart from this, water is being polluted by human activities, urbanization and industrialization. The lack of safe and unreliable drinking water constitutes the health problems for human life. Most of the human diseases are due to polluted or non-purified water resources. Desalination of salt water and impure water is suitable solution that can help reduce current and future water scarcity [1].

Energy is an important factor for every country all over the world. There are many different types of desalination processes for desalting water systems using energy. The use of fossil fuels in energy provision should not continue for everyday life because they can be exhausted and polluted to water resources and environment. Solar energy is one of the effective solution to environment pollution, the largest source of renewable energy, and abundantly available in all parts of the earth. It has some benefits in the remote areas, where there is no access to electricity or difficult to reach fossil fuels. The cost of utilizing solar energy to produce fresh water is reasonable and there is also no remained pollutant from the process. Water treatment process utilizing the solar energy for desalination technology enables human beings to acquire clean water supply with the simplest and economical way possible. Solar desalination has only recently emerged as a promising renewable energy-powered technology for producing fresh water. Solar desalination can improve health standards, because solar distilled water is chemically pure. Therefore, solar desalination is one of the simplest applications for water purification system [3].

Solar still is widely used in the solar desalination process. Purifying water through distillation is a simple yet effective means of providing drinking water in a reliable and cost-effective manner. Solar distillation could offer a real and effective solution for families in remote arid areas to clean their water supplies on-site. Solar still has been proven to be the best solution to solve water problem in these locations. It is a very simple solar device used for converting the available brackish or waste water into the potable water. This device can be fabricated easily with available materials. Solar still production is a function of solar energy (insolation) and ambient temperature. Solar stills effectively eliminate all water borne pathogens, salts, and heavy metals, and produce ultrapure water that is proven to be superior to most commercial bottled water sources [5]. The maintenance is also cheap and no skilled labour is required to

make it. But the productivity of it is very low. To increase the productivity of solar still, solar still can be integrated with flat plate collector, evacuated tube collector, parabolic trough collector, etc.

In this work, salt gradient solar pond (SGSP) is selected to supply an extra thermal energy to the basin of solar still because it is a new technique for thermal desalination and can store the solar thermal energy for a long time. Comparison is made between the solar still coupled with salt gradient solar pond as well as passive solar still.

## II. LITERATURE SURVEY

Many techniques have been developed for purification of water. Among these water purification systems, solar desalination proves to be economical and eco-friendly technique. Fedali Saida, Bougriou Cherif (2010), presents the thermal analysis of passive solar still. Mathematical equations for water, absorber, glass and insulator temperatures yield and efficiency of single slope basin have been derived. The analysis is based on the basic energy balance for the solar still. A computer model has been developed to predict the performance of the solar still. The calculations indicated that the wind speed has an influence on the glass cover temperature. It was noted that in sunshine duration, temperature of various components of the distiller follows the evolution of solar radiation [4]. Eric Spooner and Lisa Van Bladeren discussed Solar Distillation in Rajasthan, India (2013). This paper aims to guarantee that the solar still can be easily adopted and employed. The materials used to build the still are available at local markets in the city of Jodhpur and are relatively inexpensive. The solar still that they designed and built produced roughly one to two liters of water per square meter of glass surface per day [13].

A number of efforts have been made to develop and improve the performance of solar desalination systems particularly solar stills. The efficiency of the still is directly proportional to the inlet water temperature to still. To increase the temperature of the water inside the still, some researchers suggested coupling the still to solar collectors such as flat plate collector, evacuated tube collector, parabolic trough collector, solar pond, etc. Solar ponds have been studied by many researchers in the US, Israel, Australia and several other countries because of their excellent heat collection and storage performances. Experimental works basically concentrate on design, application and experimental thermal measurements in solar ponds to investigate the thermal behaviour of various types of solar ponds in different dimensions [20]. The mathematical formulation of the behaviour of solar ponds was first given by Weinberger. Theoretical studies are particularly focused on modelling of solar ponds for their performance analysis and predicting temperature variations in the ponds. Solar energy is absorbed by a solar pond from its surrounding during the day and stored in the form of heat energy in it. During the nights, due to non-existence of solar energy, no contribution is made to the pond's thermal energy [11]. The use of numerical methods for studying the solar pond was first suggested by Tabor; however, Hull first used the finite difference method to investigate solar pond performance [12].

Theoretical modeling of solar pond and integration with desalination was studied by Ibrahim Alenezi (2012). Time-dependent steady state model has been developed to predict the behavior of solar pond temperatures. Coupling a solar pond with a desalination unit could assist providing fresh potable water to the inhabitants [11]. K. Shanmugasundaram (2014) presented experimental analysis of double slope single basin solar still coupled with shallow solar pond. The performance of the double slope solar still coupled with and without shallow solar pond has been analyzed experimentally. The distilled water output and efficiency of solar still when coupled with shallow solar pond is found to be higher than solar still without coupled solar pond [18]. A. M. Dalave (2016) discussed about the experimental investigation for performance enhancement of solar still using solar pond. Solar still is the best option for the domestic purpose to get the distilled water. The productivity can be enhanced by integrating solar still with solar pond [21]. Yunes Mogheir (2017) presented about the treatment of desalination brine using an experimental solar pond. The brine characteristics were studied by using shallow solar pond SSP. Evaporation rate increases with decreasing the mirror's angle that makes with horizontal. The best performance of the pond can be achieved when the mirrors are employed as reflectors [23].

Single basin solar still was tested at our laboratory, Mechanical Engineering Department in Mandalay Technological University. Phye., P. P. have also designed temperature dependent correlations for internal heat transfer coefficients between water and glass cover of solar still. The inclination of single basin solar still was selected by theoretical and numerical result. According to the results, the optimum inclination angle is 20° [22]. However, any studies about solar pond technology and experiment have not been carried out locally. This research work aims to build an experimental, numerical and theoretical model for active solar still to test the thermal performance behavior. The single basin solar still integrated with salt gradient solar pond is proposed to improve its productivity. All the results are compared together to reach to the best operating conditions that can be used in future for solar still augmentation for the production of drinking water. In this paper, a three-dimensional two-phase model was developed for condensation and evaporation process in single slope solar still and three-dimensional model of SGSP with in-pond heat exchanger was also developed using ANSYS CFX software. The simulation results are compared with the theoretical and experimental data.

## III. THEORETICAL ANALYSIS

Theoretical analysis is being made to find out the solar radiation behavior and temperature of solution in solar pond and solar still at every instant.

**A. Solar Radiation Behavior**

The amount of solar radiation is a function of many factors like position of sun, time of day, location, distance travelled by light, and wavelength range of solar spectrum. The total solar radiation incident on a tilted surface was considered to include three components: beam, isotropic diffuse, and solar radiation diffusely reflected from the ground. It can be calculated as

$$I_T = I_b \cos \theta_i + I_d \left( \frac{1 + \cos \beta}{2} \right) + I_h \rho_{\text{ground}} \left( \frac{1 - \cos \beta}{2} \right) \tag{1}$$

The total solar radiation incident on a horizontal surface, often referred to as global radiation on the surface can be calculated as

$$I_h = I_b \cos \theta_z + I_d \tag{2}$$

The absorbed radiation in the body of water can be converted into useful thermal energy. The solar radiation intensity at depth  $x$ , in the solution is given by Beer's law as

$$I(x) = (1 - \alpha)(1 - \beta) I_h e^{-\mu x} \tag{3}$$

The beam radiation under clear sky conditions on the horizontal surface can be calculated as

$$I_b = I_{0,\text{eff}} \left[ a_0 + a_1 \exp \left( \frac{-k}{\cos \theta_z} \right) \right] \tag{4}$$

The clear sky diffuse radiation on the horizontal surface can be calculated as

$$I_d = [0.271 I_{0,\text{eff}} - 0.294 I_b] \cos \theta_z \tag{5}$$

Effective solar constant varies with the time of year according to the formula,

$$I_{0,\text{eff}} = I_0 \left( 1 + 0.033 \cos \frac{360 n}{365} \right) \tag{6}$$

The incidence angle for the horizontal surface is the zenith angle of the sun. Solar Zenith ( $\theta_z$ ) is the angle between the vertical and the line to the sun. The solar zenith angle  $\theta_z$  is of the form,

$$\cos \theta_z = \cos \phi \cos \delta \cos \omega + \sin \phi \sin \delta \tag{7}$$

The incidence angle of the sloped surface due northern hemisphere is

$$\cos \theta_i = \cos(\phi - \beta) \cos \delta \cos \omega + \sin(\phi - \beta) \sin \delta \tag{8}$$

**B. Single Basin Single Slope Solar Still**

The performance of a solar still can be predicted by writing energy balance equations on various components of the still. The heat transfer in solar still can be classified as internal and external heat transfer. The heat transfer from water surface to inner surface of glass cover taken place within the solar still is called internal heat transfer which is mainly due to convection, radiation and evaporation. The external heat transfer is mainly governed by conduction, convection and radiation processes, which are independent of each other, these are, the heat lost from the glass cover to outside atmosphere and the heat lost from basin water to outside atmosphere through the bottom and sides insulation. The details of various heat transfers in solar still are shown in Figure 1.

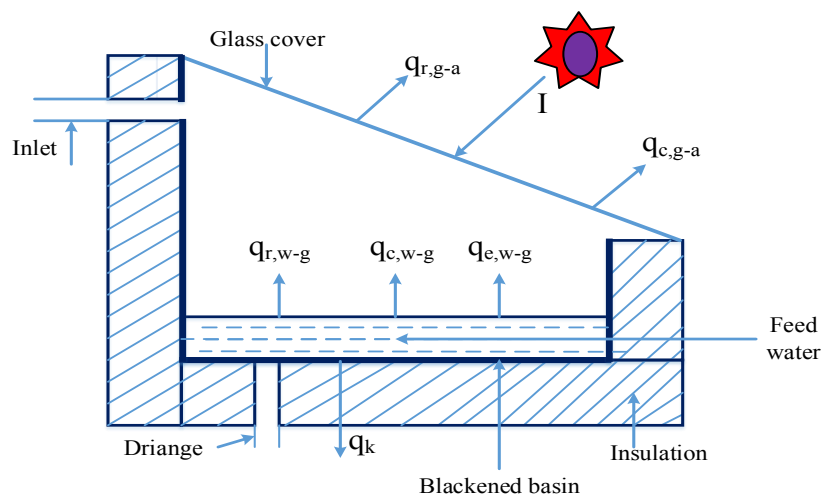


Figure 1. Heat Flux Relations in a Solar Still [1]

Energy received by the water in the still from sun is equal to the summation of energy lost by convective heat transfer between water and glass, radiative heat transfer between water and glass, evaporative transfer between water and glass, conductive heat loss from water basin, and energy gained by the water. An energy balance on the water in the basin can be written as,

$$q_{in} - q_{loss} = q_u \tag{9}$$

$$I\alpha_w - (q_{r,w-g} + q_{c,w-g} + q_{e,w-g} + q_{k,b} + q_{k,s}) = m_w c_{p,w} \left( \frac{dT_w}{dt} \right) \tag{10}$$

$$T_w^{t+\Delta t} = T_w^t + \frac{\Delta t}{m_w c_{p,w}} (I\alpha_w - q_{r,w-g} - q_{c,w-g} - q_{e,w-g} - q_{k,b} - q_{k,s}) \tag{11}$$

Energy gained by the glass cover (from sun and convective, radiative and evaporative transfer from water to glass) is equal to the summation of energy lost by convective heat transfer between glass and atmosphere, radiative heat transfer between glass and atmosphere, and energy gained by the glass. An energy balance on the cover can be written as,

$$(I\alpha_g + q_{r,w-g} + q_{c,w-g} + q_{e,w-g}) - (q_{r,g-a} + q_{c,g-a}) = m_g c_{p,g} \left( \frac{dT_g}{dt} \right) \tag{12}$$

$$T_g^{t+\Delta t} = T_g^t + \frac{\Delta t}{m_g c_{p,g}} (I\alpha_g + q_{r,w-g} + q_{c,w-g} + q_{e,w-g} - q_{r,g-a} - q_{c,g-a}) \tag{13}$$

The radiative heat transfer between water and glass is given by,

$$q_{r,w-g} = h_{r,w-g} (T_w - T_g) \tag{14}$$

The radiative heat transfer coefficient between water and glass is given by,

$$h_{r,w-g} = 0.9 \sigma (T_w^4 - T_g^4) \tag{15}$$

The convective heat transfer between water and glass is given by,

$$q_{c,w-g} = h_{c,w-g} (T_w - T_g) \tag{16}$$

The convective heat transfer coefficient between water and glass is given by,

$$h_{c,w-g} = 0.884 \left[ (T_w - T_g) + \left( \frac{P_w - P_g}{268.9 \times 10^3 - P_w} \right) T_w \right]^{1/3} \tag{17}$$

$$P_w = \exp \left( 25.317 - \frac{5144}{T_w} \right) \tag{18}$$

$$P_g = \exp \left( 25.317 - \frac{5144}{T_g} \right) \tag{19}$$

The evaporative heat transfer between water and glass is given by,

$$q_{e,w-g} = h_{e,w-g} (T_w - T_g) \tag{20}$$

The evaporative heat transfer coefficient between water and glass is given by,

$$h_{e,w-g} = \frac{16.27 \times 10^{-3} h_{c,w-g} (P_w - P_g)}{(T_w - T_g)} \tag{21}$$

The conduction heat loss from basin water to outside atmosphere through the bottom can be computed as follow;

$$q_{k,b} = U_b (T_w - T_a) \tag{22}$$

$$U_b = \frac{1}{R_b} = \frac{k A_b}{t_b} \tag{23}$$

The conduction heat loss from basin water to outside atmosphere through the sides insulation can be computed from the following simple relation:

$$q_{k,s} = U_s (T_w - T_a) \tag{24}$$

$$U_s = U_b \times \frac{A_s}{A_b}, (U_s \approx 0 \text{ as } A_s \approx A_b) \tag{25}$$

The radiative heat transfer between glass and ambient is given by,

$$q_{r,g-a} = \epsilon_g \sigma (T_g^4 - T_{sky}^4) \tag{26}$$

The convective heat transfer between glass and ambient is given by,

$$q_{c,g-a} = h_{c,g-a} (T_g - T_a) \tag{27}$$

The convective heat transfer coefficient between glass and ambient is given by,

$$h_{c,g-a} = 2.8 + 3.8 v \tag{28}$$

By analogy between heat and mass transfer, the mass transfer rate can be written as,

$$m_D = \frac{q_{e,w-g} \times A}{h_{fg}} \tag{29}$$

$$h_{fg} = 2.4935 \times 10^6 \times (1 - 9.4779 \times 10^{-4} T_v + 1.3132 \times 10^{-7} T_v^2 - 4.7974 \times 10^{-9} T_v^3) \tag{30}$$

Where,  $T_v = \frac{T_w + T_g}{2}$

The objective of still design is to maximize  $q_{e,w-g}$ , the transport of absorbed solar radiation to the cover-condenser by water vapor, as this is directly proportional to still productivity  $m^o_D$ . The still output is measured by the evaporation-condensation transfer from water basin to cover.

Daily efficiency is obtained by the output of the single basin solar still and divided by the input of the solar basin solar still.

$$\text{Daily Efficiency} = \left[ \frac{\text{Output}}{\text{Input}} \right] \times 100 \tag{31}$$

Increase in efficiency of solar still is defined as the difference between the output of single basin solar still with and without modifications divided by output of single basin solar still without modification.

$$\text{Increasing Efficiency} = \left[ \frac{\text{Output}_{\text{With SP}} - \text{Output}_{\text{Without SP}}}{\text{Output}_{\text{Without SP}}} \right] \times 100 \tag{32}$$

### C. Salt Gradient Solar Pond

The performance of a solar pond depends substantially on the amount of solar energy that is inputted into the solar pond and the amount of heat loss from the pond. A solar pond is a non-homogeneous system in which various heat transfer processes occur. The input and output heat values passing through the upper zone of a solar pond can be briefly described as in Figure 2. The net heat in the surface layer is thermally fed by the solar irradiation and the conducted heat from the lower zones but part of this heat may be mainly lost by the mentioned four processes. The upper convective zone is assumed to have a uniform temperature  $T_u$ .

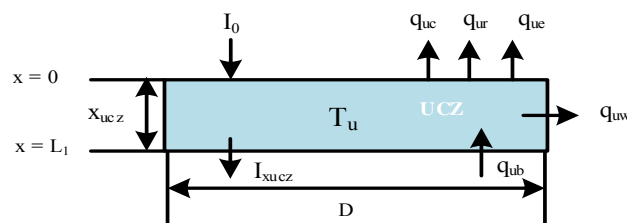


Figure 2. Energy balance for UCZ

The energy balance equation can be written as:

$$q_{in} - q_{loss} = q_{store} \tag{33}$$

$$(I_0 + q_{ub}) - (I_u + q_{Loss}) = \rho C_p x_{ucz} \frac{\partial T_u}{\partial t} \tag{34}$$

The heat balance of UCZ in non-differential form can be written as

$$k \left. \frac{\partial T(x, t)}{\partial t} \right|_{x=x_{ucz}} + I_0 - I_u - q_{Loss} = \frac{\rho C_p x_{ucz}}{\Delta t} (T_u^{t+\Delta t} - T_u^t) \tag{35}$$

The temperature distribution for UCZ is given as

$$T_u^{t+\Delta t} = T_u^t + \frac{\Delta t}{\rho C_p x_{ucz}} \left[ I_0 - I_u - q_{Loss}^t + k \frac{(T_i^t - T_u^t)}{\Delta x} \right] \quad (36)$$

The total heat loss from pond's surface can be calculated as follows:

$$q_{loss} = q_{uc} + q_{ur} + q_{ue} + q_{uw} \quad (37)$$

Convection heat transfer from the upper layer to the atmosphere depends mainly on the wind speed and the temperature difference between the atmosphere and the water surface; this can be expressed as in the following equation:

$$q_{uc} = h_c (T_u - T_a) \quad (38)$$

The heat transfer between the upper zone and the sky is a function of the ambient and water surface temperatures. Thus, the radiation heat loss equation may be written as the following:

$$q_{ur} = \sigma \epsilon_w [T_u^4 - T_k^4] \quad (39)$$

$$T_k = T_a - (0.55 + 0.061 \sqrt{P_a})^{0.25} \quad (40)$$

The evaporation heat loss includes the wind heat transfer coefficient and the vapour and partial pressure of water.

$$q_{ue} = \left( \frac{\lambda h_c}{1.6 C_a P_{atm}} \right) (P_u - P_a) \quad (41)$$

$$P_u = \exp \left( 18.403 - \frac{3885}{T_u + 230} \right) \quad (42)$$

$$P_a = (RH) \exp \left( 18.403 - \frac{3885}{T_a + 230} \right) \quad (43)$$

The rate of heat loss through the upper layer wall of pond can be calculated as,

$$q_{uw} = U \Delta \theta / A \quad (44)$$

The NCZ layer on the energy balance equation is solved by dividing the equal sub-layer. In this layer heat coming from  $i+1$  layer and leaving to  $i-1$  layer both by conduction. The input and output heat values passing through the middle zone of a solar pond can be briefly described as in Figure 3.

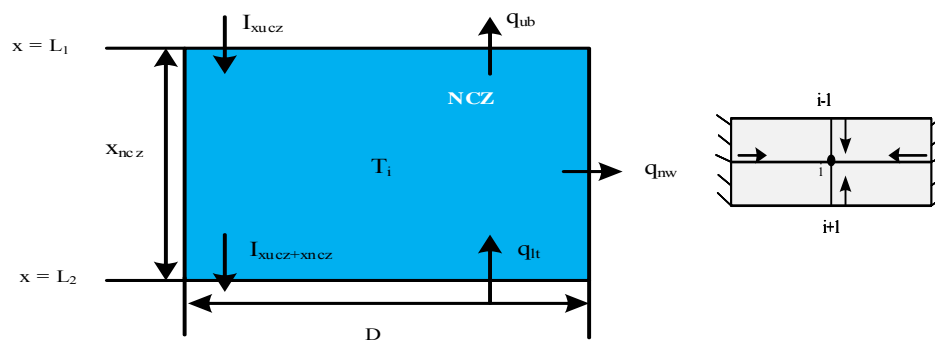


Figure 3. Energy balance for NCZ

The energy balance of this zone can be written as:

$$\left( I|_{x=i-1} + q_{cond3} \right) - \left( I|_{x=i+1} + q_{cond2} + q_{nw} \right) = \rho C_p \Delta x \frac{\partial T_i}{\partial t} \quad (45)$$

The heat balance of NCZ in non-differential form can be written as

$$k \frac{\partial T(x, t)}{\partial t} \Big|_{x=i+1} - k \frac{\partial T(x, t)}{\partial t} \Big|_{x=i-1} + I|_{x=i-1} - I|_{x=i+1} = \frac{\rho C_p \Delta x}{\Delta t} (T_i^{t+\Delta t} - T_i^t) \quad (46)$$

The temperature distribution for NCZ is given as

$$T_i^{t+\Delta t} = T_i^t + \frac{\Delta t}{\rho C_p \Delta x} \left[ I \Big|_{x=i-1} - I \Big|_{x=i+1} + k \frac{(T_{i+1}^t - T_i^t)}{\Delta x} - k \frac{(T_i^t - T_{i-1}^t)}{\Delta x} \right] \quad (47)$$

The input and output heat values passing through the lower zone of a solar pond can be briefly described as in Figure 4. The lower convective zone is assumed to have a uniform temperature  $T_L$ .

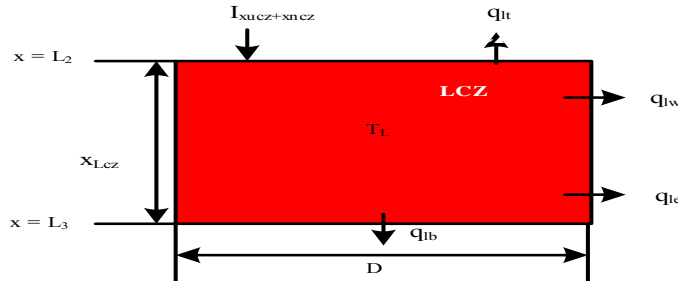


Figure 4. Energy balance for LCZ

The energy balance of this zone can be written as:

$$I_{Xucz+Xncz} - (q_{Lt} + q_{le} + q_{lb} + q_{lw}) = \rho C_p x_{LCZ} \frac{\partial T_L}{\partial t} \quad (48)$$

The heat balance of LCZ in non-differential form can be written as

$$-k \frac{\partial T(x,t)}{\partial x} \Big|_{x=x_{lcz}} + I_{Xucz+Xncz} = \frac{\rho C_p x_{LCZ}}{\Delta t} (T_L^{t+\Delta t} - T_L^t) \quad (49)$$

The temperature distribution for LCZ is given as

$$T_L^{t+\Delta t} = T_L^t + \frac{\Delta t}{\rho C_p x_{LCZ}} \left[ I_{Xucz+Xncz} - k \frac{(T_L^t - T_i^t)}{\Delta x} \right] \quad (50)$$

#### IV. NUMERICAL ANALYSIS

Computational Fluid Dynamics (CFD) approach was used to study the temperature distribution in the single basin solar still. Geometric model of solar still is created using ANSYS CAD module and this geometric model is imported to the ANSYS meshing module to generate the meshing. The geometry has six faces which are considered as impermeable wall. The vertical higher and lower heights of the unit are 0.46 m and 0.13 m which results in a top surface slope of 20°. The width and length of the unit are 0.86 m and 1.22 m. In the mesh generation 6144 nodes, 4991 elements are generated. Figure 5 shows a three-dimensional (3D) model of single slope solar still based on data available in experimental set up of solar still and Figure 6 shows the meshing structure of single basin solar still.

The mesh files of solar still are imported to the ANSYS CFX 15 which solves the equations of continuity, momentum and energy. To simulate the condensation and evaporation process in solar still appropriate boundary conditions must be specified at each boundary. In CFX Pre, physics and boundary conditions are applied on the domain to solve the mass and momentum equation. The recorded experimental data are for eight hours, starts from 9 am to 5 pm. Here ANSYS CFX run time of 8 hours that is required for modeling of solar still which is in an unsteady state process. Hence, to overcome this problem, it assumes that steady state condition is reached after time period of 1 hour and received water; glass temperatures inside basin are constant.

A two-phase domain is created in VOF frame work for liquid water and mixture of water vapor and air. Evaporation process is modeled as laminar, accounting for thermal energy heat transfer while considering the effects of buoyancy. Due to distinct interface between liquid and vapor phase, both phases are assumed to be continuous. Two resistance models are taken to transfer heat, zero resistance model for gas phase and heat transfer coefficient for water phase. It was assumed that bottom temperature is equal to water temperature. The bottom and top surfaces are at fixed temperatures and the remaining side walls are assumed adiabatic so there is no heat loss to surrounding. No slip boundary condition is specified for liquid phase and free slip boundary condition is specified for

vapor phase. For producing droplets on the condensing cover plates, it assumes that adhesion forces are taken into account in simulation. The water and gas mixture volume fraction are taken as 0.21 and 0.79 respectively.

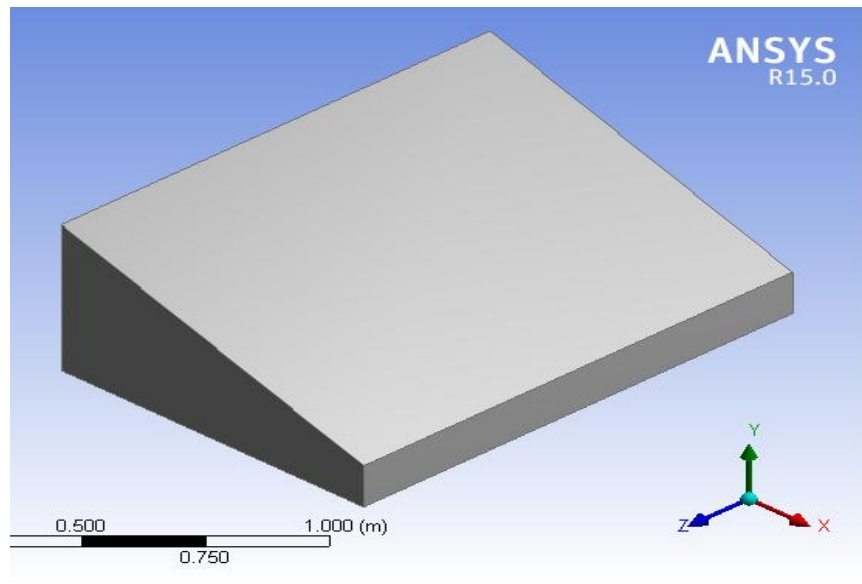


Figure 5. Three-dimensional model of Single Basin Solar Still

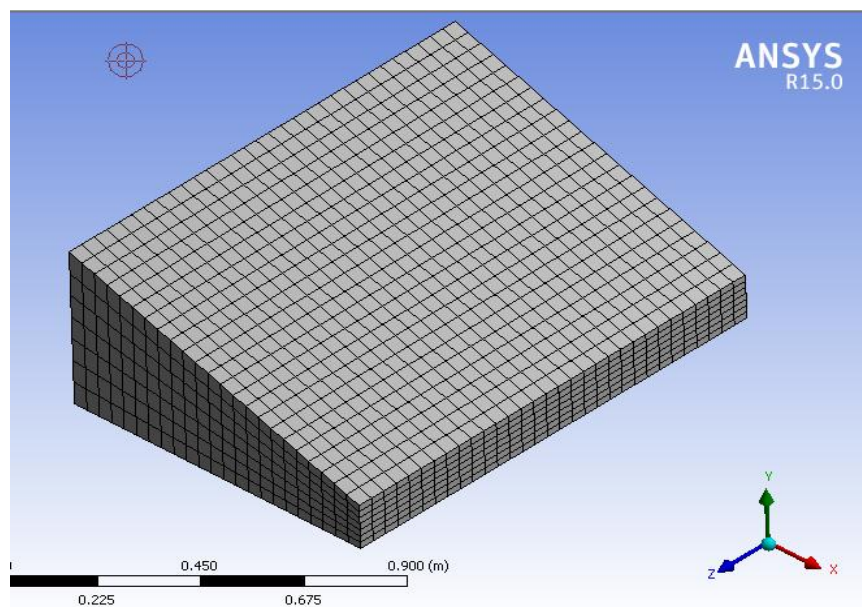


Figure 6. Mesh Generation of Single Basin Solar Still

The commercial software ANSYS was used for the CFD numerical simulation of temperature distribution in a salt gradient solar pond. Firstly, three-dimensional geometry models for solar pond are drawn in ANSYS Workbench which allows for the use of CAD geometries or to build the geometry using a number of geometry tools. The cylindrical domain of consideration is that of the existing pond dimensions with 1.04 m diameter and 1.2 m height. The pond has been divided in three zones. The bottom zone (LCZ) has 0.48 m depth. The middle zone (NCZ) has 0.6 m depth and five equally divided sub-layers, each 0.12 m depth. The top zone (UCZ) has 0.12 m depth. Therefore, the physical domain consists of seven layers. And then, the 3D geometric model of in-pond heat exchanger is created using Auto-CAD software and this geometric model is imported to the middle of SGSP in ANSYS Workbench. After that, meshing is done in the ANSYS meshing approach. The number of mesh nodes is 207500 and elements 1086200. Figure 7 shows a three-dimensional model of SGSP with in-pond heat exchanger and Figure 8 shows the meshing structure of this model.

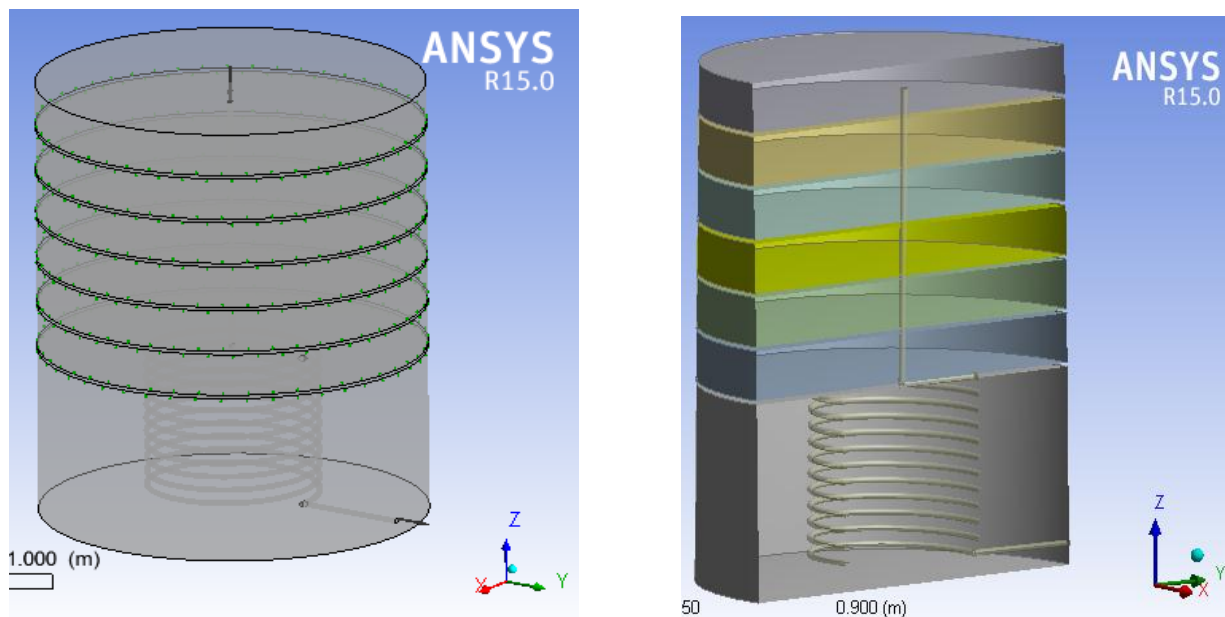


Figure 7. Three-dimensional model of SGSP with in-pond heat exchanger

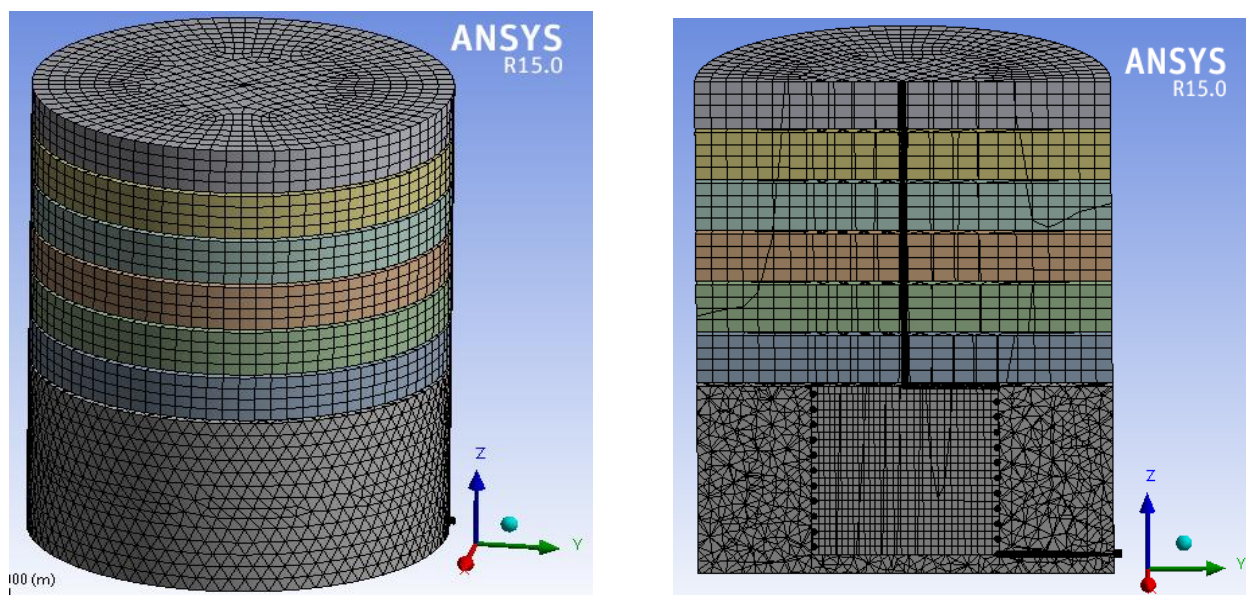


Figure 8. Mesh Generation of SGSP with in-pond heat exchanger

The mesh files are imported to ANSYS CFX-15 software. In ANSYS CFX-Pre, the properties of the domains are defined along with their interface properties. The gravitational acceleration was set as  $9.81 \text{ m/s}^2$ . The fluid motion was considered as laminar flow, since water velocity didn't achieve greater magnitudes. Bottom and vertical walls of the pond are set to be impermeable and thermally insulated. Also, the top surface is taken to be at ambient temperature according to local meteorological data. Modelling of the physics included creating interfaces for flow zones, assigning boundary conditions, assigning initial conditions, applying governing equations with appropriate models and choosing the flow materials. The solution control and declaration of variables were also done in the ANSYS CFX-Pre. The problem presented in this simulation consists in solving the combined equations of Navier-Stokes and energy equation for compressible fluid and subjected to density and concentration variation with temperature. After solving the governing equations in solver, the results of CFD simulation are showed in CFD-Post.

Three-dimensional CFD simulation is performed for temperature distribution in a salt gradient solar pond by using ANSYS CFX software. A complete workflow for CFD simulation is presented in Figure 7.

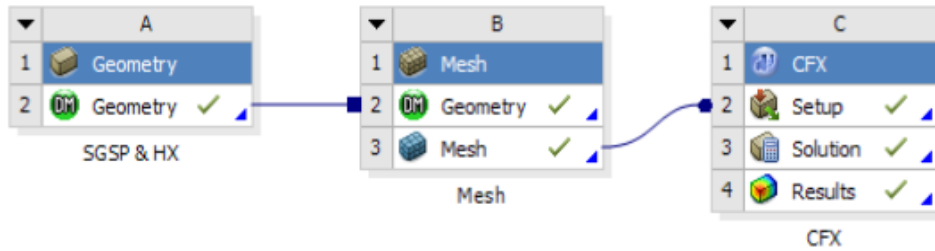


Figure 7. CFD Numerical Simulation Procedure

### V. EXPERIMENTAL SETUP

The experiment mainly consists of two parts namely, single basin single slope solar still and salt gradient solar pond. The experimental setup of single basin single slope solar still is shown in Figure 8. The single basin single slope solar still is made up of mild steel sheet. The still basin is painted with matt black color to increase solar absorption. It is placed inside the plywood box which is made of plywood sheet at front and back heights of 0.2 m and 0.53 m, and size of 1.22 m × 0.86 m. The space between box and basin is filled with polystyrene foam sheet as an insulation purpose to reduce the heat losses from the bottom and the side walls of the solar still. A 5-mm thick glass is used as roof as well as the condensing surface in the still. The glass has been mounted at an angle of 20° equal to the latitude of Mandalay, to ensure maximum transmission of solar radiation into the still. The edges of the glass are sealed so that the entire basin becomes airtight. A collection trough is made in the still to collect the distilled water. The collection tray is used to drain the fresh water to an external beaker. An inlet PVC hose is fixed at the rear wall of the still for feeding raw water and hot water from solar pond. Two thermocouples were installed to measure the glass inside temperature and water temperature. The four-legged wood stand is appropriate to construct the solar still (height 1.2 m and size 1.2 m × 0.82 m). Four robust casters should be fixed at the end of each leg to facilitate moving and orientation of solar still.

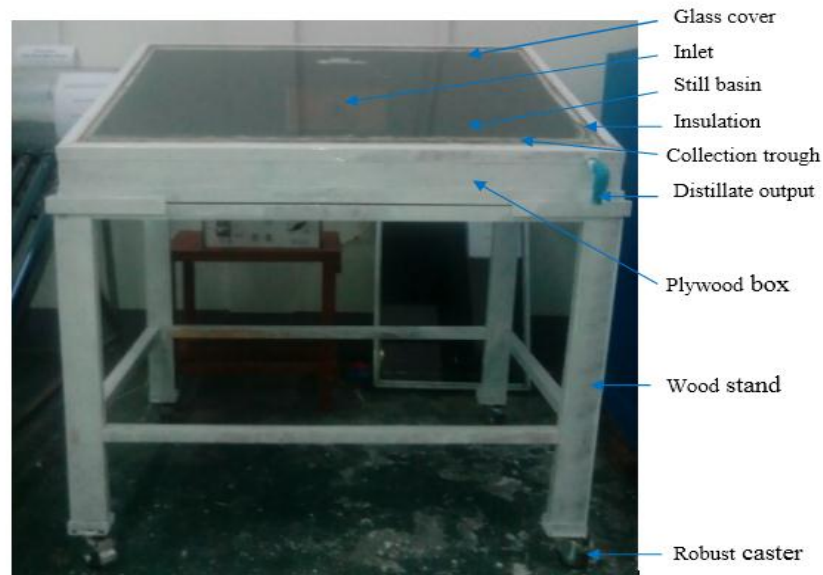
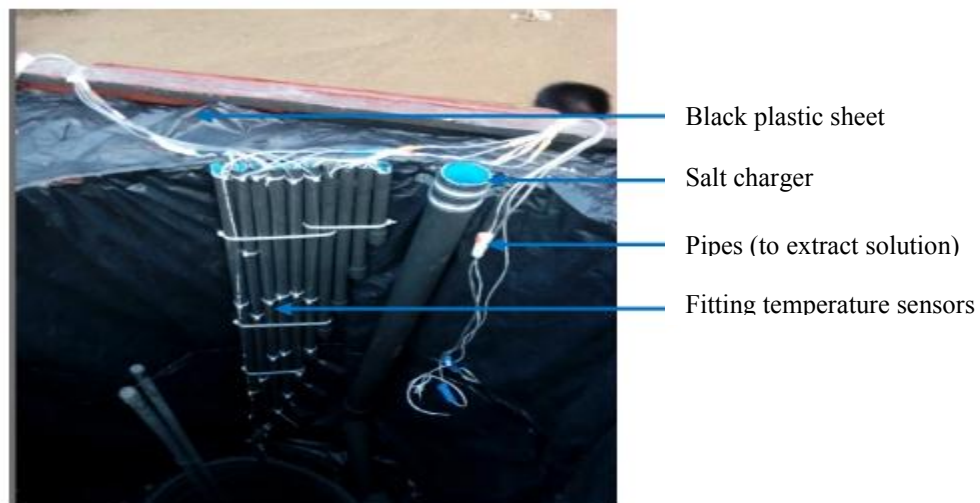
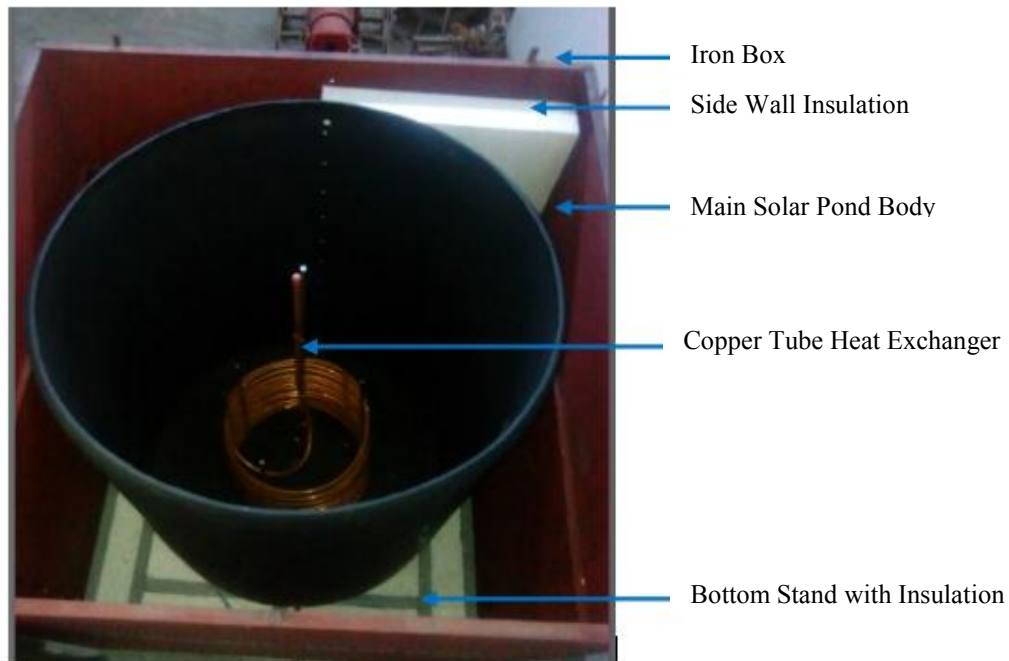


Figure 8. Photographic View of Experimental Set up of Solar Still

The above said solar still is integrated with a SGSP. The experimental setup of salt gradient solar pond is shown in Figure 9. The main solar pond body is made up of cylindrical shape polyethylene water tank of 1000 L volume, 1.04 m diameter, 1.29 m height and 10 mm thick. The inner and outer surfaces of it are painted with matt black color to increase the absorption of incident solar radiation. It is enclosed in an iron box which is made of iron sheet at a height of 1.65 m and size of 1.32 m × 1.32 m. The inner and outer surfaces of box are painted with red oxide to avoid corrosion. The tank's wall was insulated with polystyrene foam sheets of 0.14 m thickness. The bottom of solar pond was supported by an iron stand insulated with polystyrene foam sheets of 0.3 m thickness. Plywood is used to cover the insulation and covered with black plastic. The copper tube of 16 mm diameter is used as a straight and coil heat exchanger and stainless steel solid rod is used to stand the heat exchanger in the middle of pond. To measure the temperature

distributions in each layer, the ten digital thermometers are used. The PVC pipes and lips of 12 mm diameter are used to insert the temperature sensors for each layer. The PVC pipe of 76 mm diameter is used to make the salt charger. The solution from the pond is piped to measure the salt concentration of each layer. If the salt lost from the bottom zone, the require amount of salt can add to the salt charger without destroying the various layers. All temperature sensors, salt charger and pipes are fixed to the inside wall of the pond. The secondary plastic tank of 200 L capacity is used to supply the fresh/ salt water to the main solar pond. The four-legged iron stands are appropriate to construct the main solar pond (height 1.52 m and size 1.32 m × 1.32 m) and secondary tank (height 3.66 m and size 0.61m × 0.61 m) stands. The eight concrete stands are used to make the strong based frames and then installed with iron stands. The top of solar pond is covered by 8 mm thick transparent glass with aluminum frame. The iron ladder is used to observe the temperature distribution of solar pond. A diffuser can be made of plastic pipe in circular form and several holes along them led the higher density brine out. It is an essential role for filling process. Pure sodium chloride salt ( $\text{NaCl} \geq 98.5\%$ ) is used to establish the salt gradient layer. The flow of water from plastic tank to pond can be controlled by flexible hose and valve. Single-phase submersible pump of 35 m head, 6 m<sup>3</sup>/h flows and 2860 rpm speed are used to supply the solution to the secondary tank. There are three zones in the SGSP. The top zone is the Upper Convection Zone (UCZ) and consists of the fresh water. The middle zone is the Non-Convection Zone (NCZ) and consists of five sub-layers in which each sub-layer is heavier and hotter than the ones above it. This density gradient prevents the heat loss from the lower zone to the upper zone. The bottom zone is the Lower Convection Zone (LCZ) and consists of highest salt concentration. This zone acts as the heat storage zone and thermal energy can be extracted from this zone. The SGSP is connected with solar still by a pipe through a flow control valve.



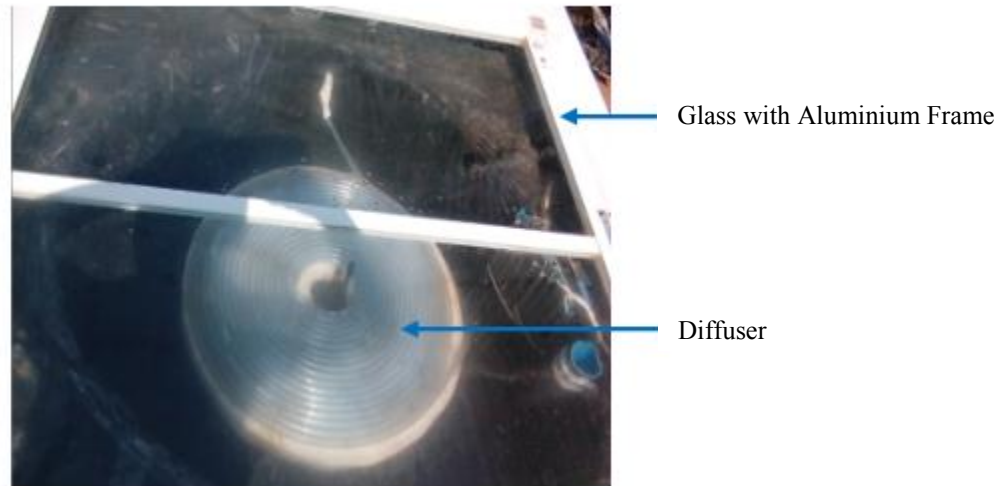


Figure 9. Photographic View of Experimental Set up of Salt Gradient Solar Pond

The experimental procedure is as follows. The schematic diagram and photographic view of solar still is integrated with solar pond as shown in Figure 10 and 11. When the solar radiation falls on the surface of the SGSP, the heat penetrates through UCZ and NCZ to be stored at the LCZ. Water from top layer of solar pond (UCZ) is allowed to pass through NCZ and LCZ by a copper tube. While passing through LCZ, the water absorbs the heat from LCZ and gets heated. This preheated water is sent to solar still through a flow control valve. The depth of water in solar still is taken as 20 mm. The incident solar radiation is transmitted through the glass cover of solar still and absorbed by the water in the basin. Thus, the basin water gets heated up and evaporates. The evaporated water particles condense in the inside layer of the glass cover. This condensed water flows down the cover due to the slope provided and reaches the channels, where it is collected by the collection jar leaving behind the salts, minerals, and most other impurities, including germs. The evaporated water in the solar still is compensated by the hot water from the solar pond. The decrease in water level in the solar pond is also compensated by gently adding (without disturbing the three zones) fresh water on the top side of the solar pond.



A measurement system had been installed for recording the experimental data. The digital thermometers with stainless steel sensor probe were used to measure the temperature of the various zones in the solar pond, basin water and glass cover in the solar still. Solar radiation is measured with solar power meter. Wind velocity is measured by a digital anemometer. Infrared thermometer is used to measure the glass outside temperature. Thermometer is used to measure the ambient temperature. The amount of produced potable water is measured by a collection tank of one-liter capacity and 250 ml measuring cylinder. Salt meter and hydrometer are used manually to measure the salt concentration and density of the liquids samples. Readings are taken for every one hour between 8:00 am and 5:00 pm. Figure 12 shows the measuring instruments.



Figure 12. Measuring Instruments (a) Digital Thermometer, (b) Solar Power Meter, (c) Digital Anemometer, (d) Thermometer, (e) Infrared Thermometer, (f) 250 ml Measuring Cylinder, (g) Salt Meter, (h) Hydrometer

## VI. RESULTS AND DISCUSSION

The performance of the single basin single slope solar still integrated with and without salt gradient solar pond has been analyzed theoretically, numerically and experimentally. Energy balance equations have been solved analytically for the temperature elements of the solar still and solar pond. ANSYS CFX software is used for numerical analysis. A number of experimental tests are performed to predict the still performance at Mechanical Engineering Department in Mandalay Technological University, Myanmar. The following results were obtained.

Computational Fluid Dynamics approach was used to study the temperature distribution in the single basin solar still. Model geometry and meshing were done using ANSYS Workbench 15. Attention in made to concentrate on the temperature distribution of still basin. Simulation was carried out for one hour with all initial conditions. The temperature distribution of water and gas mixture, superficial velocity and mass fraction of gas mixture of single basin solar still integrated with and without salt gradient solar pond are shown in Figure 13 to 20.

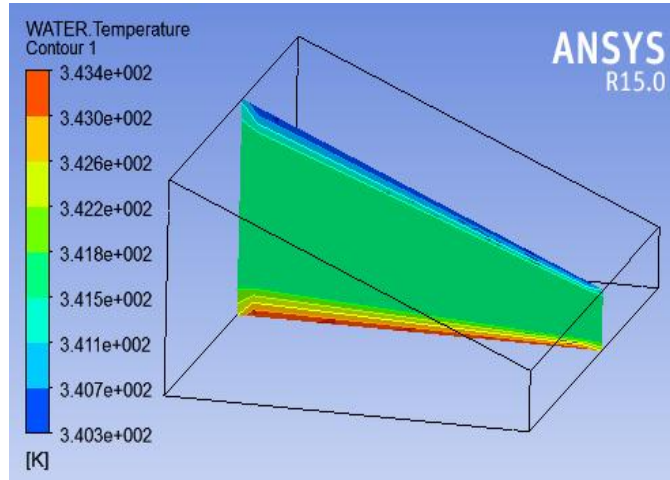


Figure 13. Water temperature distribution of Solar Still with SGSP (21.9.2017)

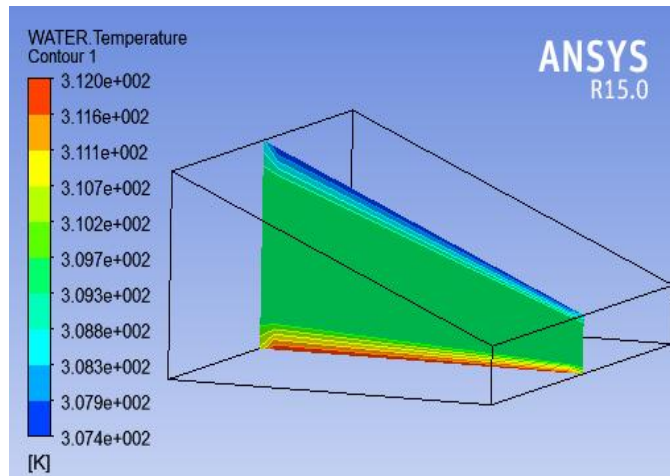


Figure 14. Water temperature distribution of Solar Still without SGSP (21.9.2017)

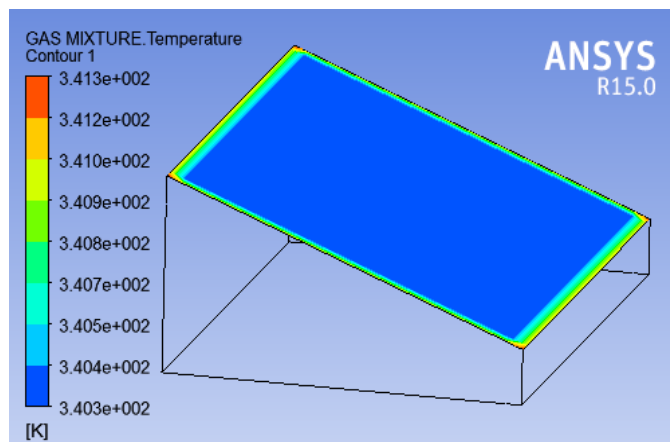


Figure 15. Gas Mixture temperature distribution of Solar Still with SGSP (21.9.2017)

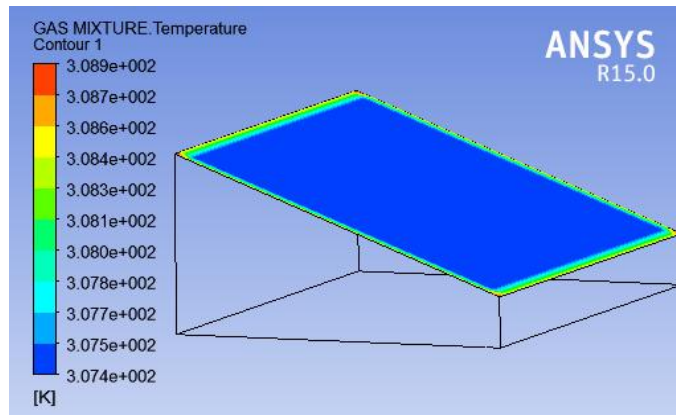


Figure 16. Gas Mixture temperature distribution of Solar Still without SGSP (21.9.2017)

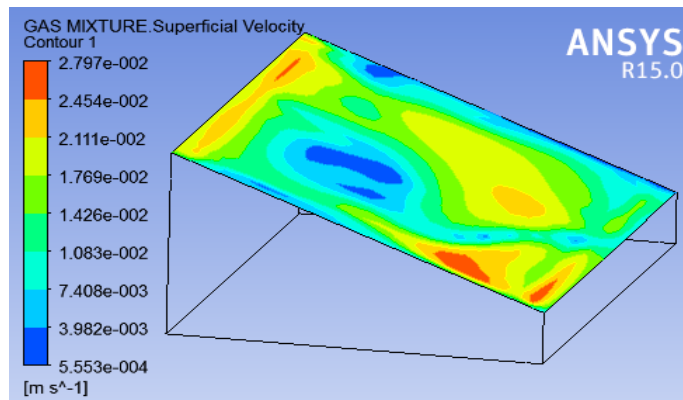


Figure 17. Gas Mixture Superficial Velocity of Solar Still with SGSP (21.9.2017)

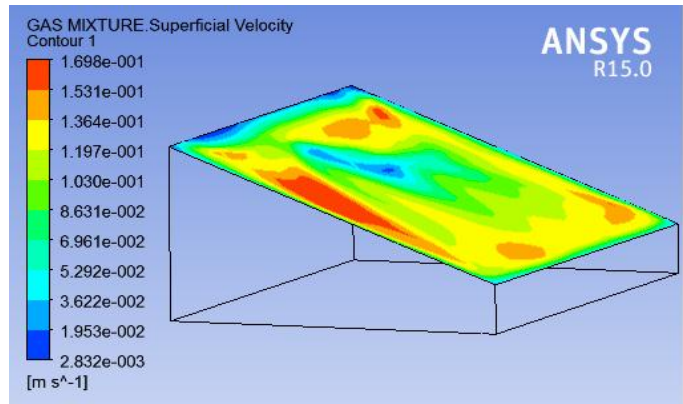


Figure 18. Gas Mixture Superficial Velocity of Solar Still without SGSP (21.9.2017)

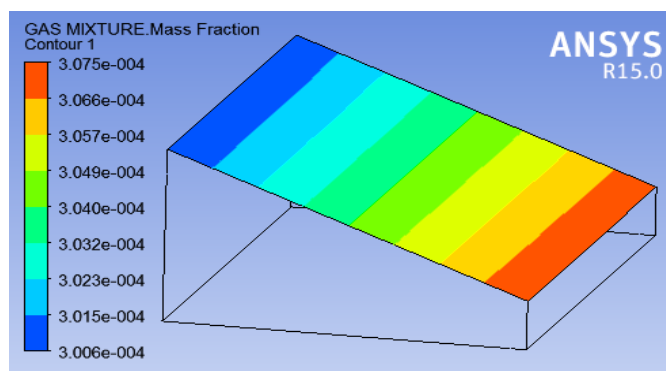


Figure 19. Gas Mixture Mass Fraction of Solar Still with SGSP (21.9.2017)

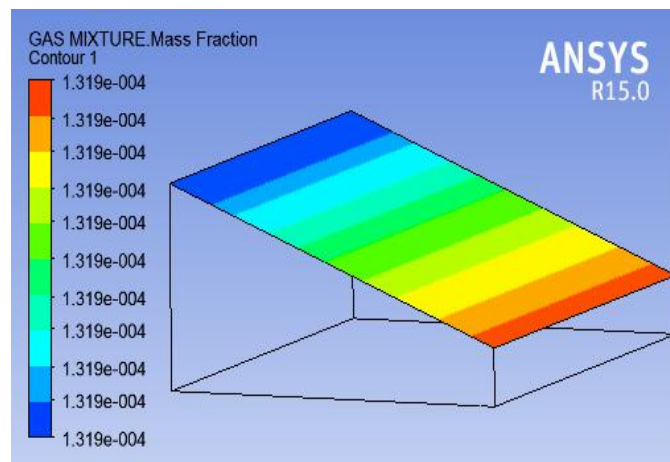


Figure 20. Gas Mixture Mass Fraction of Solar Still without SGSP (21.9.2017)

After the post-processing of simulation results, the temperature distribution of SGSP is obtained and presented in the Figure 21. In three dimensional simulation, the total depth of solar pond is analyzed. It is already possible to visualize the thermal stratification in a solar pond. The different colours defined the value of temperature in each zone of solar pond. It can be seen that temperature in UCZ remains approximately the same with ambient temperature. Temperature distribution in NCZ increases with depth similar to the density gradient. The highest temperature is reached in LCZ and this heat can store in the bottom of SGSP.

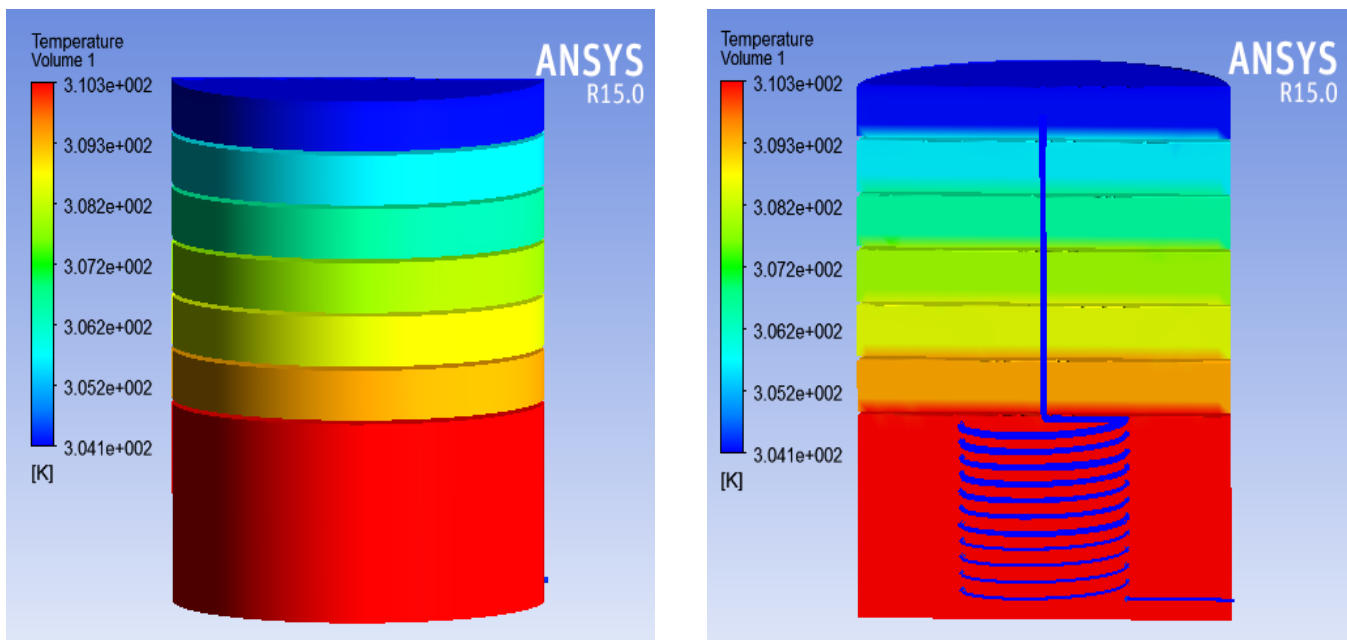


Figure 21. Temperature Distribution of SGSP (21.9.2017)

The experiment of the salt gradient solar pond was carried out using solar energy without using auxiliary heater from January to October 2017. After performing the filling process, the temperature distribution inside the pond was measured manually with ten digital thermometers distributed vertically with a gap around 6 cm. Daily data was observed once an hour from 8 am until 5 pm. According to the experimental result, SGSP has been able to operate properly by the increase of temperature at 5 pm on every day, although there is still a decreasing in temperatures that occurs in the next morning due to heat loss from the sides and bottom of the tank at night. Therefore, the data for average temperature at the bottom (LCZ) layer of SGSP at 5 pm is shown in Figure 22. There are variances in the figure, the stored temperature started at the time due to pond filling preparations, and salt concentration arrangements, which last several days, collecting and storing solar energy as heating energy mode, which increased storage region temperatures. The temperature differences increased with time to reach its maximum value. Solar pond heats up slowly but store heat in a longer period of time. It can be seen that the maximum storage temperature reaches 312 K.

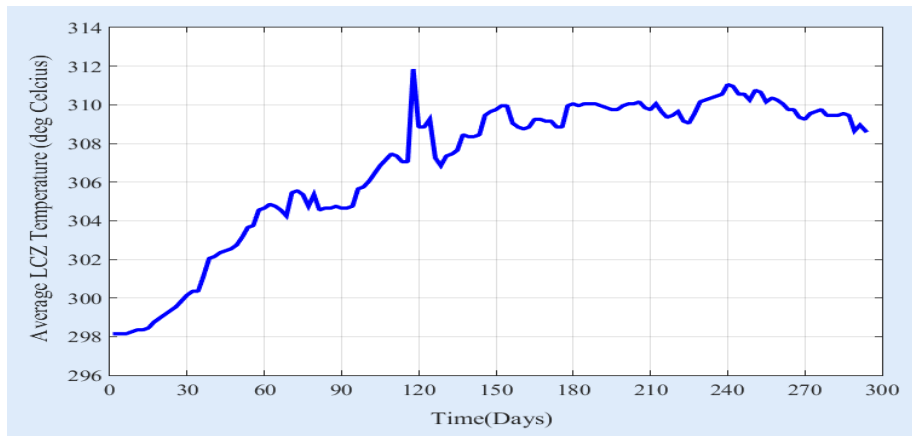


Figure 22. Average solution temperature rises of SGSP (16/1/2017 to 31/10/2017)

The variation of water temperature from heat exchanger tube immersed in SGSP has been depicted in Figure 23. The extraction of heat from the SGSP by water through the heat exchanger tube is moderate and it gradually increases. The maximum water temperature is found to be 50 °C and heat energy extracted from pond water is given as input to the still throughout the working hours of the day to enhance the evaporation rate in the still.

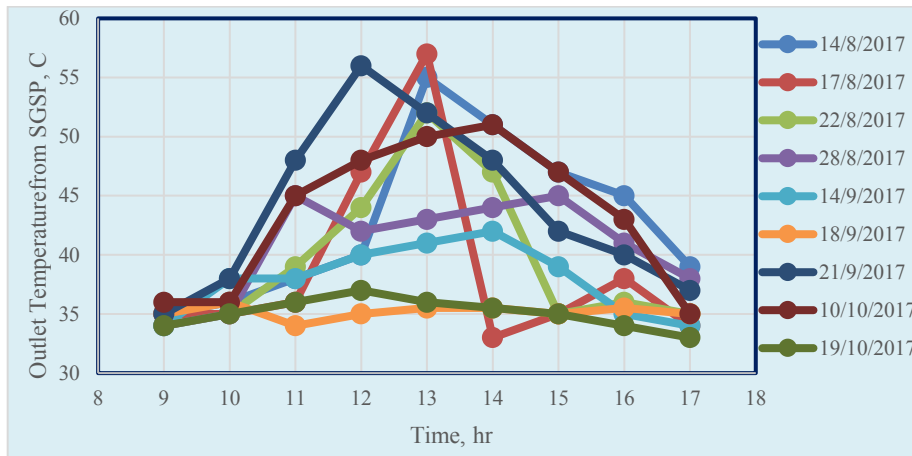


Figure 23. Variations of temperature of the pond water for the experimental days

The temperature variations depend on the solar energy that reaches on the surface, the climate conditions of the place and time. The hourly variations of solar radiation on the pond and still with respect to time are shown in Figure 24 and 25. From these figures, it is observed that the solar radiation intensity is gradually increased and reaches maximum during 12 pm to 1 pm and then decreased gradually. The maximum value of the solar radiation is 1258 W/m<sup>2</sup>.

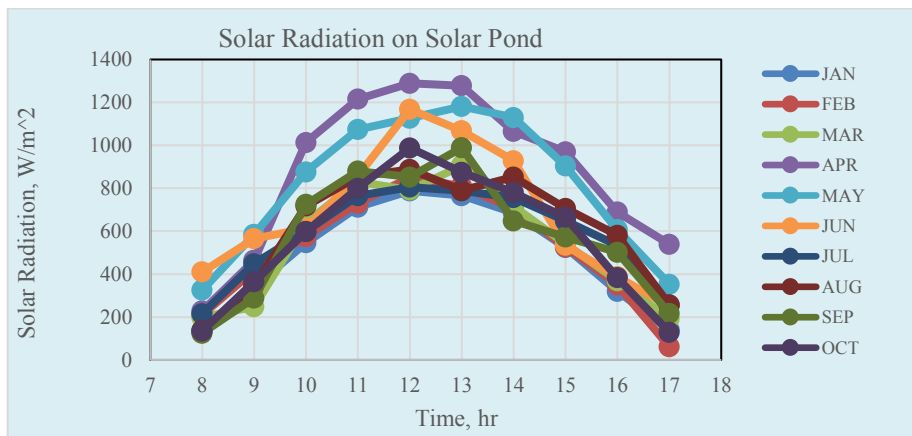


Figure 24. Variations of the solar radiation intensity on Salt Gradient Solar Pond with time

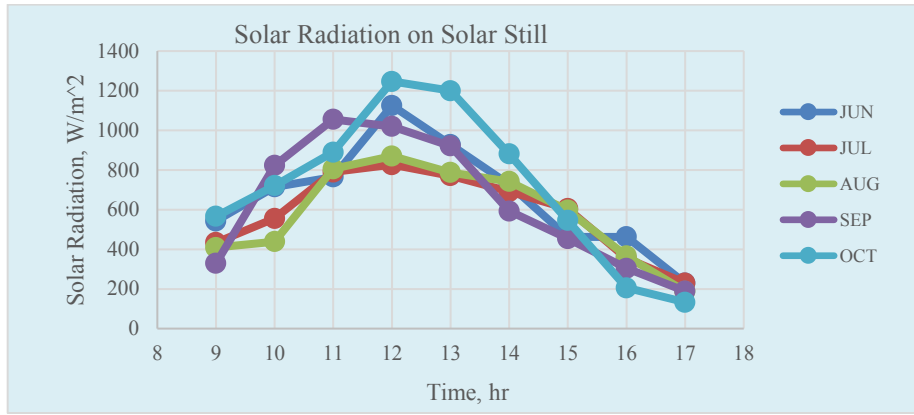


Figure 25. Variations of the solar radiation intensity on Single Basin Solar Still with time

Figure 26 shows the variation of ambient temperature with respect to time. It can be observed that the maximum ambient temperature (36°C) is obtained during the period from 11 a.m. to 3 p.m.

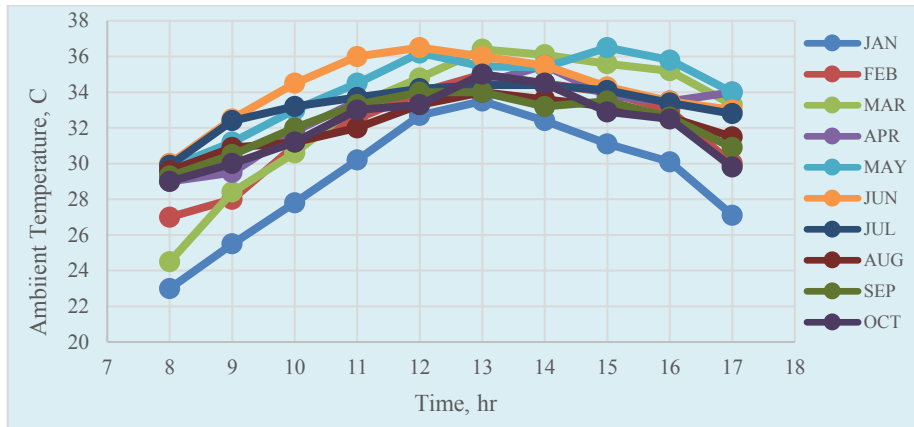


Figure 26. Variations of the ambient temperature and time

The productivity of the solar still can be augmented by preheating the inlet water. This can be done by a solar pond. A salt gradient solar pond is connected with the solar still by a flow control valve. The effect of SGSP coupled with solar still is compared with simple solar still and the results are shown in Figure 27 and 28. It shows that, the productivity of the salt gradient solar still is much higher than the solar still alone throughout the day. The additional heat energy supplied from SGSP increases the basin water temperature in the still. This leads to higher productivity in the salt gradient solar still. It is found that, the productivity of the salt gradient solar still is 40.78% higher than the simple solar still.



Figure 27. Comparisons of distilled water output of the still with and without SGSP

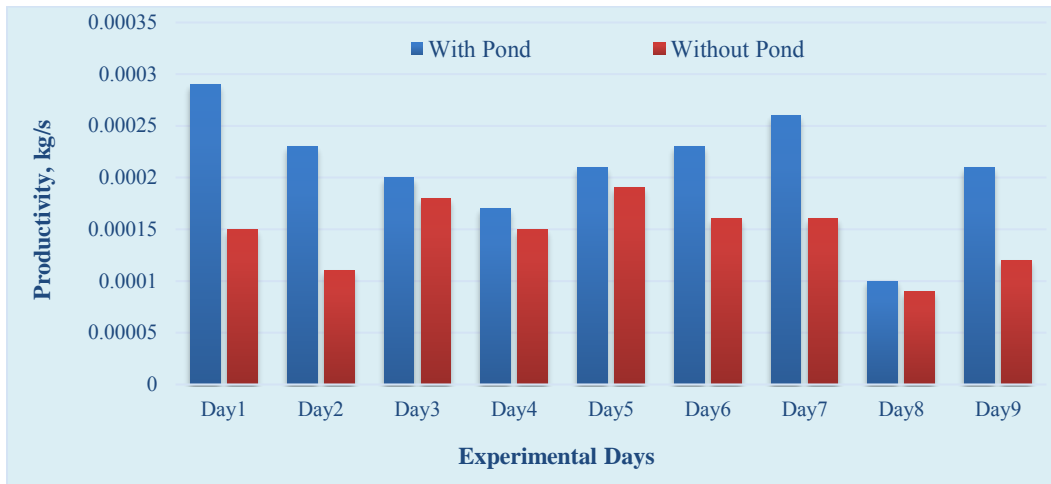


Figure 28. Comparisons of distilled water output of the still with and without SGSP

Figure 29 shows the comparison of PH level of solar still with and without SGSP. It shows that, the PH level of the salt gradient solar still is much higher than the solar still alone.

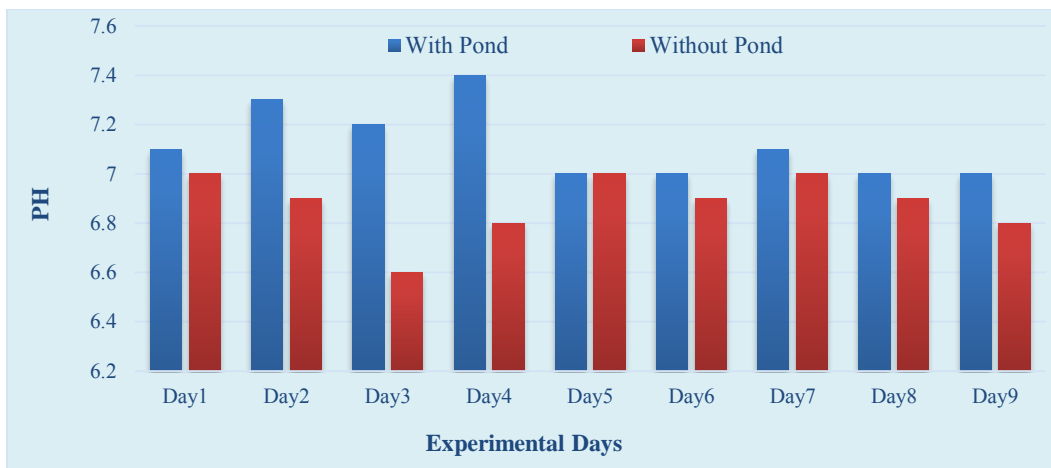


Figure 29. Comparisons of PH level of distilled water output of the still with and without SGSP

Figure 30 shows the productivity of distilled water from the single basin single slope solar still with and without salt gradient solar pond on September 21<sup>st</sup> 2017 as determined by experimental measurements, theory calculation and numerical simulation model. It is found that the theoretical and numerical results are in good agreement with the experimental results.

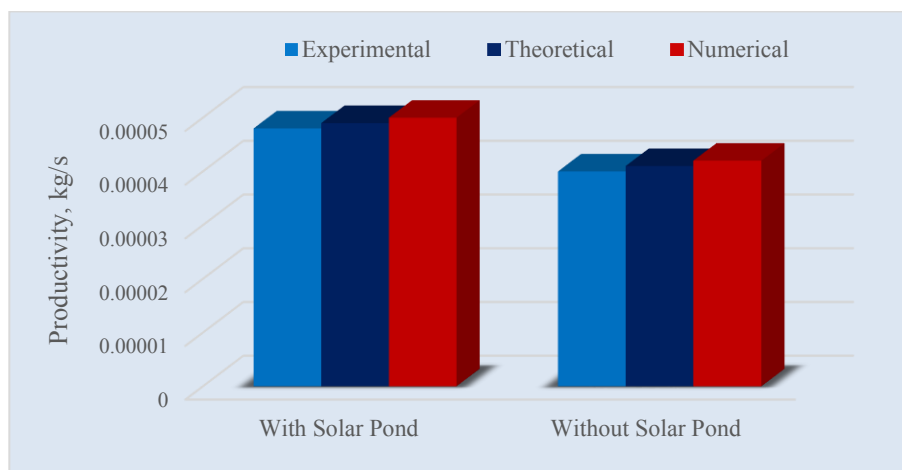


Figure 30. Theoretical and experimental values of distilled water output with coupled SGSP

## VII. CONCLUSIONS

The solar still can be used as a water purifier for domestic purposes by using solar energy. Solar-pond technology is the renewable and efficient technology for pre-heating the inlet water to solar still. A salt gradient solar pond was used to store the solar thermal energy and the heat energy stored by the solar pond was used for preheating water in single basin solar still. Experiments of single basin solar still were carried out with and without solar pond. The experiment is performed from 9 am to 5 pm at Mechanical Engineering Department, Mandalay Technological University. Here we have focused on the use of salt gradient solar pond to increase the daily productivity of single basin single slope solar still. In this work, solar evaporation of water is simulated using ANSYS CFX. CFD prediction results become insignificantly closer to the theoretical and experimental work. The maximum pH level is 7.4 with integration and 7 without integration and the minimum pH level is 7 with integration and 6.6 without integration. The maximum water temperature is obtained about 95°C and 72°C with and without integration. The maximum yield of the still is about 1.5 liters and 1.1 liters with and without integration. The productivity of solar still with solar pond was 40.78 % more than solar still alone. The performance of the solar still integrated with the salt gradient solar pond provides better performance compared with the still without integration.

## ACKNOWLEDGEMENTS

The author would like to acknowledge the support and encouragement of Dr. Sint Soe, Rector of Mandalay Technological University. The author is very thankful to Dr. Htay Htay Win, Professor and Head of Department of Mechanical Engineering, M.T.U, for her invaluable help, and indispensable guidance in the preparation of this paper. The author wishes to express her deepest special thanks to her supervisor, Dr. Myat Myat Soe, Professor, Department of Mechanical Engineering, M.T.U, for her enthusiastic instruction, invaluable input into the present research as well as for her understanding and moral support throughout the course of this challenging study. The author is thankful to Japan International Cooperation Agency (JICA), Project for Enhancement of Engineering Higher Education (EEHE) for supporting the experimental facilities. The author would like to thank all teachers from Mechanical Engineering Department, Mandalay Technological University for their kindness, graceful, attitude and permission to do this paper. The author wishes to express her heartfelt thanks to her parents for their guidance and encouragements to attain her destination without any trouble.

## NOMENCLATURE

Symbols	Descriptions	Units
$a_0, a_1$	Coefficient of beam radiation	-
$C_{pw}$	Specific heat capacity of water	kJ/kgK
$C_{pg}$	Specific heat capacity of glass	kJ/kgK
$h_c$	convective heat transfer coefficient	W/m <sup>2</sup> K
$h_{r,w-g}$	Radiative heat transfer coefficient between water and glass	W/m <sup>2</sup> K
$h_{c,w-g}$	Convective heat transfer coefficient between water and glass	W/m <sup>2</sup> K
$h_{e,w-g}$	Evaporative heat transfer coefficient between water and glass	W/m <sup>2</sup> K
$h_{r,g-a}$	Radiative heat transfer coefficient between glass and ambient	W/m <sup>2</sup> K
$h_{c,g-a}$	Convective heat transfer coefficient between glass and ambient	W/m <sup>2</sup> K
$h_{fg}$	Latent heat of vaporization of water	W/m <sup>2</sup> K
$I_0$	Solar constant	W/m <sup>2</sup>
$I_b$	Beam irradiance	W/m <sup>2</sup>
$I_d$	Diffuse irradiance	W/m <sup>2</sup>
$I_h$	Total solar radiation incident on a horizontal surface	W/m <sup>2</sup>
$I_T$	Total solar radiation incident on a tilted surface	W/m <sup>2</sup>
$I_{0,eff}$	Effective solar constant	W/m <sup>2</sup>
$k$	Thermal conductivity	W/mK
$m_w$	Mass flow rate of water	kg/s
$m_g$	Mass flow rate of glass	kg/s
$n$	number of days of the year	-
$p_w$	water vapor partial pressure at water temperature	
$p_g$	water vapor partial pressure at glass temperature	
$p_u$	water vapor pressure as at upper layer temperature	Pa
$p_a$	water vapor partial pressure in ambient temperature	Pa
$q_{r,w-g}$	Radiative heat transfer between water and glass	W/m <sup>2</sup>
$q_{c,w-g}$	Convective heat transfer between water and glass	W/m <sup>2</sup>
$q_{e,w-g}$	Evaporative heat transfer between water and glass	W/m <sup>2</sup>

$q_{r,g-a}$	Radiative heat transfer between glass and ambient	$W/m^2$
$q_{c,g-a}$	Convective heat transfer between glass and ambient	$W/m^2$
$q_{k_s,b}$	Conduction heat loss to the bottom	$W/m^2$
$q_{k_s,s}$	Conduction heat loss to the sides	$W/m^2$
$q_u$	useful energy stored in the pond	$W/m^2$
$q_{ub}$	heat gained from bottom in upper zone	$W/m^2$
$q_{lb}$	heat loss from the bottom of pond	$W/m^2$
$q_{lt}$	heat loss from the top	$W/m^2$
$q_{le}$	heat loss by heat extraction	$W/m^2$
$q_{uw}$	heat loss from the sidewalls in UCZ	$W/m^2$
$q_{nw}$	heat loss from the sidewalls in NCZ	$W/m^2$
$q_{lw}$	heat loss from the sidewalls in LCZ	$W/m^2$
$T_a$	Ambient temperature	$^{\circ}C$
$T_u$	upper layer temperature	$^{\circ}C$
$T_i$	gradient layer temperature	$^{\circ}C$
$T_L$	lower layer temperature	$^{\circ}C$
$T_k$	sky temperature	$^{\circ}C$
$T_w$	Water temperature	$^{\circ}C$
$T_g$	Water temperature	$^{\circ}C$
$t$	operating time	hr
$\alpha$	Reflectance of radiation at surface	-
$\beta$	Collector's tilt angle	degree
$\epsilon_w$	Emissivity of water	-
$\delta$	Solar declination angle	degree
$\theta_z$	Solar zenith angle	degree
$\theta_i$	Solar incidence angle	degree
$\mu$	Attenuation or extinction coefficient	-
$\phi$	Latitude of the location	-
$\sigma$	Stefan – Boltzman constant	-
$\rho$	density	$kg/m^3$

REFERENCES

- [1] Velmurugan,V; Mugundhan, K. ‘*Experimental Studies on Solar Stills Integrated with a Mini Solar Pond*’, Proceedings of the 3rd BSME-ASME International Conference on Thermal Engineering, 20-22 December, 2006, Dhaka, Bangladesh.
- [2] Velmurugan, V. ‘*Solar Stills Integrated with a Mini Solar Pond — Analytical Simulation and Experimental Validation*’, Desalination 216 (2007) 232–241.
- [3] Velmurugan,V; Mandlin, J; Stalin, B. ‘*Augmentation of Saline Streams in Solar Stills Integrating with a Mini Solar Pond*’, Desalination 249 (2009) 143–149.
- [4] Fedali Saida, Bougriou Cherif, “*Thermal Analysis of Passive Solar Still*”, 2010.
- [5] Srithar, K. ‘*Performance Analysis of Vapor Adsorption Solar Still Integrated with Mini-solar Pond for Effluent Treatment*’, International Journal of Chemical Engineering and Applications, Vol. 1, No. 4, December 2010 ISSN: 2010-0221.
- [6] Sampathkumar, K; Arjunan, T., V. ‘*Active Solar Distillation—A Detailed Review*’, Renewable and Sustainable Energy Reviews 14 (2010) 1503–1526.
- [7] Gowtham, M; Chander, M., S. ‘*Augmentation of Saline Streams by Concentrated Solar Distiller with Mini Solar Pond*’, International Journal of Environmental Science and Development, Vol. 2, No. 3, June 2011.
- [8] Panchal, H., P. ‘*Modelling and verification of single slope solar still using ANSYS-CFX*’, International Journal of Energy and Environment, Volume 2, Issue 6, 2011 pp.985-998.
- [9] Tanaka, H. ‘*Tilted Wick Solar Still with Flat Plate Bottom Reflector*’, Desalination 273 (2011) 405–413.
- [10] Ali, M., I.; Joseph, B. ‘*Performance Investigation of Solar Still Integrated to Solar Pond*’, Bonfring International Journal of Power Systems and Integrated Circuits, Vol. 2, No. 1, March 2012.
- [11] Ibrahim Ienezi : ‘*Salinity Gradient Solar Ponds: Theoretical Modelling and Integration with Desalination*’, Chemical Engineering, Faculty of Engineering and Physical Sciences, University of Surrey, May 2012.
- [12] Aizaz, A. ‘*Construction and Analysis of a Salt Gradient Solar Pond for Hot Water Supply*’, European Scientific Journal, vol.9, No.36, December 2013.
- [13] Eric Spooner and Lisa VanBladeren, “*Solar Distillation in Rajasthan, India*”, 2013.

- [14] Shanmugasundaram, K; Janarthanan, B. '*Performance Analysis of the Single Basin Double Slope Solar Still Integrated with Shallow Solar Pond*', International Journal of Innovative Research in Science, Engineering and Technology, ISSN: 2319-8753, Vol. 2, Issue 10, October 2013.
- [15] Hunashikatti, P., T.; Suresh, K., R. '*Development of Desalination Unit Using Solar Still Coupled with Evacuated Tubes for Domestic Use in Rural Areas*', CURRENT SCIENCE, VOL. 107, NO. 10, 25 NOVEMBER 2014.
- [16] Kanan, S. '*A Simple Heat and Mass Transfer Model for Salt Gradient Solar Ponds*', The University of Manchester, UK, IJMAIMME, Vol.8, No. 1, 2014.
- [17] PATEL, H., B.; SONI, U., R. '*Performance Analysis of Active Solar Still with ETHP Solar Collator Attached as Natural Convection*', International Journal on Recent and Innovation Trends in Computing and Communication, Volume: 2 Issue: 5, May 2014, Available @ <http://www.ijritcc.org>
- [18] Shanmugasundaram, K. '*Experimental Analysis of Double Slope Single Basin Solar Still Coupled With Shallow Solar Pond*', International Journal of Frontiers in Science and Technology, ISSN 2321 – 0494, vols. 2, no. 1, 2014.
- [19] Singh, A. '*Simulation of single slope solar still at different inclinations using CFD*', International Journal of Advance Research and Innovation, Volume 2, Issue 2 (2014) 407-413 ISSN 2347 - 3258 .
- [20] Vora, S., H. '*Experimental Study on a Portable Mini Salt Gradient Solar Pond*', Journal of Alternate Energy Sources and Technologies (JoAEST), Volume 6, Issue 3, 2015.
- [21] Dalave, A., M. '*Experimental Investigation for Performance Enhancement of Solar Still using Solar Pond*', International Journal for Research in Applied Science & Engineering Technology (IJRASET), Vol.4, Issue 1, January 2016.
- [22] Phyo, P., P. '*Design and Performance of Solar Water Distillation System*', Mechanical Engineering Department, Mandalay Technological University, September 2016.
- [23] Mogheir, Y. '*Treatment of Desalination Brine Using an Experimental Solar Pond*', Journal of Engineering Research and Technology, Volume 4, Issue 1, March 2017.

#### AUTHORS

**First Author** – Ni Ni Aung, Ph.D. candidate, Mandalay Technological University, angelkalay123@gmail.com

**Second Author** – Myat Myat Soe, Professor, Mandalay Technological University, myatmyatsoe.mtu @gmail.com.